UNCLASSIFIED

SECURITY CLASSIFICATION OF THIS PAGE

DTIC FILE COPY

REPORT DOCUMENTATION PAGE

Form Approved
OMB No 0704-0188
Exp Date Jun 30 1986

1a REPORT SECURITY CLASSIFICATION
UNCLASSIFIED

1b RESTRICTIVE MARKINGS

3. DISTRIBUTION/AVAILABILITY OF REPORT
Published in the open literature

AD-A196 716

5. MONITORING ORGANIZATION REPORT NUMBER(S)

DTIC ELECTE JUN 21 1988 S D

6a. NAME OF PERFORMING ORGANIZATION
Research Directorate, RD&EC
US Army Missile Command

6b. OFFICE SYMBOL (If applicable)
AMSMI-RD-RE-OP

7a. NAME OF MONITORING ORGANIZATION
same as 6a

6c. ADDRESS (City, State, and ZIP Code)
Redstone Arsenal, AL 35898-5248

7b. ADDRESS (City, State, and ZIP Code)
same as 6c

8a. NAME OF FUNDING/SPONSORING ORGANIZATION
same as 6a

8b. OFFICE SYMBOL (If applicable)

9. PROCUREMENT INSTRUMENT IDENTIFICATION NUMBER

8c. ADDRESS (City, State, and ZIP Code)
same as 6c

10. SOURCE OF FUNDING NUMBERS

PROGRAM ELEMENT NO.	PROJECT NO.	TASK NO	WORK UNIT ACCESSION NO

11. TITLE (Include Security Classification)
OPTICAL PHASE CONJUGATION WITH SMOOTH PUMP PROFILES (U)

12. PERSONAL AUTHOR(S)
Haus, J. W., Bowden, C. M., and Sung, C. C.

13a TYPE OF REPORT	13b TIME COVERED	14. DATE OF REPORT (Year, Month, Day)	15. PAGE COUNT
Open-Literature	FROM ____ TO ____	1987 April 15	8

16. SUPPLEMENTARY NOTATION
The report appeared as an open-literature publication in Physical Review A, Vol. 35, pages 3398-3405 (1987)

17 COSATI CODES		
FIELD	GROUP	SUB-GROUP

18. SUBJECT TERMS (Continue on reverse if necessary and identify by block number)
Degenerate four-wave mixing; optical phase conjugation; signal field; smooth profiles; pump profiles,

19. ABSTRACT (Continue on reverse if necessary and identify by block number)
We present analytical results for the steady-state signal and phase-conjugate fields interacting with smoothly varying nondepleted pump waves in a nearly degenerate four-wave-mixing geometry. Signal depletion is retained in the equations and we study the effect that detuning on the input signal from the degenerate pump amplitudes has on the reflected conjugate wave and the transmitted signal wave. A general result is derived for the appearance of spontaneous amplification under weak restrictions on the profile of the degenerate pump fields. The conjugation of the phase front of the signal is studied for exponential and hyperbolic secant functions multiplying the coupling coefficients and comparison is made with corresponding results for square profile pump fields. These results are discussed and their relevance to phase conjugation of pulses is examined.

20. DISTRIBUTION/AVAILABILITY OF ABSTRACT
☐ UNCLASSIFIED/UNLIMITED ☒ SAME AS RPT ☐ DTIC USERS

21. ABSTRACT SECURITY CLASSIFICATION
Uncl

22a NAME OF RESPONSIBLE INDIVIDUAL	22b TELEPHONE (Include Area Code)	22c OFFICE SYMBOL
Dr. Charles M. Bowden	(205) 876-2650	AMSMI-RD-RE-OP

DD FORM 1473, 84 MAR 83 APR edition may be used until exhausted. All other editions are obsolete.

SECURITY CLASSIFICATION OF THIS PAGE

PHYSICAL REVIEW A VOLUME 35, NUMBER 8 APRIL 15, 1987

Optical phase conjugation with smooth pump profiles

J. W. Haus
Physics Department, Rensselaer Polytechnic Institute, Troy, New York 12180-3590

C. M. Bowden
Research Directorate, Research, Development, and Engineering Center, U. S. Army Missile Command, Redstone Arsenal, Alabama 35898-5248

C. C. Sung
Department of Physics, The University of Alabama in Huntsville, Huntsville, Alabama 35899
(Received 29 September 1986)

We present analytical results for the steady-state signal and phase-conjugate fields interacting with smoothly varying nondepleted pump waves in a nearly degenerate four-wave-mixing geometry. Signal depletion is retained in the equations and we study the effect that detuning on the input signal from the degenerate pump amplitudes has on the reflected conjugate wave and the transmitted signal wave. A general result is derived for the appearance of spontaneous amplification under weak restrictions on the profile of the degenerate pump fields. The conjugation of the phase front of the signal is studied for exponential and hyperbolic secant functions multiplying the coupling coefficients and comparison is made with corresponding results for square profile pump fields. These results are discussed and their relevance to phase conjugation of pulses is examined.

I. INTRODUCTION

One of the many remarkable phenomena resulting from the mixing of electromagnetic waves in nonlinear media is optical phase conjugation.[1] It is realized in a wide range of materials and under several experimental conditions. There are new types of adaptive optical devices (called phase-conjugating mirrors) that use this phenomenon to create a scattered electromagnetic wave from the signal field, called the conjugate field. The conjugate wave propagates along the same axis as the incoming signal, but with its phase and propagating direction reversed. The conjugate waves have the property of correcting distortions in a wave front of a coherent electromagnetic field that were introduced in the signal wave as it passed through an inhomogeneous medium. Thus the conjugate wave is called the "time-reversed" analogue of the signal field.

Degenerate four-wave mixing (DFWM) is a simple method used to generate optical phase conjugation.[1] It has been proposed for a variety of applications including interferometry and signal processing.[2-4] While applications such as this are intriguing, there is a need to estimate the fidelity of the phase-conjugate wave not only with respect to the time reversal of the amplitude, but also with respect to the time reversal of the phase across the wave front.

For pulses the signal field is polychromatic and significant variation in the response of the optical phase conjugator to the components of the frequency spectrum can be expected. This expectation has motivated studies of the transient response of these devices.[5] An alternative method of studying the response of a phase conjugator is the use of steady-state signal fields which are detuned from the degenerate pump fields.[6] Of course, the results of both methods are related and they have a direct bearing on experiments.[7]

All of the above-mentioned papers endow the pump fields with a square profile. It is the purpose of this paper to deal with pump fields whose profiles are smooth. This causes, as is shown below, significant quantitative differences in the response of the phase conjugator; surprisingly, some properties are unchanged. We show, for instance, that the region of amplification of *degenerate* signal and conjugate fields is not changed when inhomogeneous pump profiles are used. On the other hand, for detuned signal fields the response of the phase conjugator is weaker for smoother pump profiles. Taken together this can lead to large quantitative discrepancies in the frequency response of the phase conjugator with different pump profiles.

In Sec. II the derivation of the equations in the slowly varying envelope approximation is given and necessary notation is introduced. Analytic results are presented and discussed in Sec. III. In Sec. IV conclusions are drawn about the results.

II. DERIVATION OF EQUATIONS

The wave equation for the electromagnetic fields in a medium with a scalar dielectric constant is

$$\nabla^2\mathbf{E}-\frac{n^2}{c^2}\frac{\partial^2\mathbf{E}}{\partial t^2}=\frac{4\pi}{c^2}\frac{\partial^2\mathbf{P}}{\partial t^2}\ , \tag{1}$$

where $\mathbf{P}$ denotes the nonlinear polarization of the medium. The linear nonresonant interactions have been eliminated and are included in the index of refraction n. $\mathbf{E}$ is the electromagnetic field and c is the speed of light in vacuum.

Several waves are mixed in the nonlinear medium. There are two counterpropagating pump fields with amplitudes, $\hat{\mathbf{E}}_{p_1}(\mathbf{x})$ and $\hat{\mathbf{E}}_{p_2}(\mathbf{x})$ and their frequencies are degenerate. These are wave vectors $\mathbf{k}_1$ and $-\mathbf{k}_1$, respectively, with $|\mathbf{k}_1| = k' = n\omega'/c$; their frequencies are degenerate. These are assumed to be strong steady-state fields compared with the signal $\hat{\mathbf{E}}_s(\mathbf{x},t)$ and conjugate $\hat{\mathbf{E}}_c(\mathbf{x},t)$ field amplitudes, which propagate along the z axis with wave vector $\mathbf{k}_s = k_s\hat{\mathbf{e}}_z$ and $\mathbf{k}_c = -k_c\hat{\mathbf{e}}_z$, respectively, where the carets denote a unit vector. The pump waves are assumed to be undepleted here. The electric field is written as the sum of these four amplitudes with appropriate plane-wave phase factors:

$$\mathbf{E}(\mathbf{x}) = [\hat{\mathbf{E}}_{p_1}(\mathbf{x})e^{i\mathbf{k}_1\cdot\mathbf{x}} + \hat{\mathbf{E}}_{p_2}(\mathbf{x})e^{-i\mathbf{k}_1\cdot\mathbf{x}}]e^{-i\omega' t} + \hat{\mathbf{E}}_s(\mathbf{x})e^{ik_s z - i\omega_s t} + \hat{\mathbf{E}}_c(\mathbf{x})e^{-ik_c z - i\omega_c t} + \text{c.c.}\,, \tag{2}$$

where c.c. refers to the complex conjugate of the first terms on the right-hand side. The polarization can also be expanded into four terms as given in Eq. (2); the slowly varying envelope approximation[8] for the amplitudes in Eq. (2) is

$$|\mathbf{k}_i\cdot\nabla\hat{\mathbf{E}}_i| \ll k^2|\hat{\mathbf{E}}_i| \quad \text{and} \quad \left|\frac{\partial\hat{\mathbf{E}}_i}{\partial t}\right| \ll \omega|\hat{\mathbf{E}}_i|\,, \tag{3}$$

where $i = p_1$, p_2, c, or s. We are only interested in the signal and conjugate field amplitudes and the equations for these fields are

$$2ik_s\left(\frac{n}{c}\frac{\partial\hat{\mathbf{E}}_s}{\partial t} + \frac{\partial}{\partial z}\hat{\mathbf{E}}_s\right) + \nabla_t^2\hat{\mathbf{E}}_s = \frac{-4\pi\omega_s^2}{c^2}\hat{\mathbf{P}}_s \tag{4a}$$

and

$$2ik_c\left(-\frac{n}{c}\frac{\partial\hat{\mathbf{E}}_c^*}{\partial t} + \frac{\partial}{\partial z}\hat{\mathbf{E}}_c^*\right) + \nabla_t^2\hat{\mathbf{E}}_c^* = \frac{-4\pi\omega_c^2}{c^2}\hat{\mathbf{P}}_c^*\,, \tag{4b}$$

where the polarization has been expanded into two modes

$$\mathbf{P} = (\hat{\mathbf{P}}_s e^{i(k_s z - \omega_s t)} + \hat{\mathbf{P}}_c e^{-i(k_c z + \omega_c t)}) + \text{c.c.}\,,$$

and the appropriate amplitude contributions appear in Eq. (4). The operator ∇_t^2 is the Laplacian in the direction transverse to the z axis.

To make explicit calculations we assume linear polarization for the signal and the conjugate field and the polarization is a linear function of $\hat{\mathbf{E}}_s$ and $\hat{\mathbf{E}}_c^*$. When the medium relaxes fast compared to electric field amplitude variations, the scalar functions for the polarizations can be represented as

$$\hat{P}_s = C_1\hat{E}_s + C_2\hat{E}_c^* \quad \text{and} \quad \hat{P}_c^* = C_3\hat{E}_c^* + C_4\hat{E}_s\,. \tag{5}$$

The coefficients (C_i) depend on the particular medium and are dependent on the amplitudes E_{p_1} and E_{p_2}.

Assuming a Kerr medium and all fields linearly polarized in the same direction, the polarization is

$$P = \chi_3 E^3\,. \tag{6}$$

Then from Eq. (2), the polarization amplitudes are

$$\hat{P}_s = 3\chi_3(|\hat{E}_{p_1}|^2 + |\hat{E}_{p_2}|^2)\hat{E}_s + 6\chi_3\hat{E}_{p_1}\hat{E}_{p_2}\hat{E}_c^* \tag{7a}$$

and

$$\hat{P}_c = 3\chi_3(|\hat{E}_{p_1}|^2 + |\hat{E}_{p_2}|^2)\hat{E}_c + 6\chi_3\hat{E}_{p_1}\hat{E}_{p_2}\hat{E}_s^*\,. \tag{7b}$$

Since the amplitudes $\hat{E}_{p_1}(\mathbf{x})$ and $\hat{E}_{p_2}(\mathbf{x})$ are not plane waves, the coupling coefficients, appearing in Eq. (4) after inserting Eqs. (7), are also functions of the spatial coordinates. This dependence is simplified by considering the signal and conjugate fields to propagate perpendicular to the pump fields and by allowing the pump fields to have a beam waist which is much larger than the transverse extent of the fields $\hat{E}_c$ and $\hat{E}_s$ (see Fig. 1). Nevertheless, the pumps still have a finite extent along the z axis and they possess a smooth profile. The equations of motion can be written as

$$2ik_s\left(\frac{n}{c}\frac{\partial\hat{E}_s}{\partial t} + \frac{\partial\hat{E}_s}{\partial z}\right) + \nabla_t^2\hat{E}_s = \alpha(z)\hat{E}_s + \beta(z)\hat{E}_c^*\,,$$
$$2ik_c\left(-\frac{n}{c}\frac{\partial\hat{E}_c^*}{\partial t} + \frac{\partial\hat{E}_c^*}{\partial z}\right) + \nabla_t^2\hat{E}_c^* = \alpha(z)\hat{E}_c^* + \beta(z)\hat{E}_s\,, \tag{8}$$

where the functions $\alpha(z)$ and $\beta(z)$ are taken as real. The

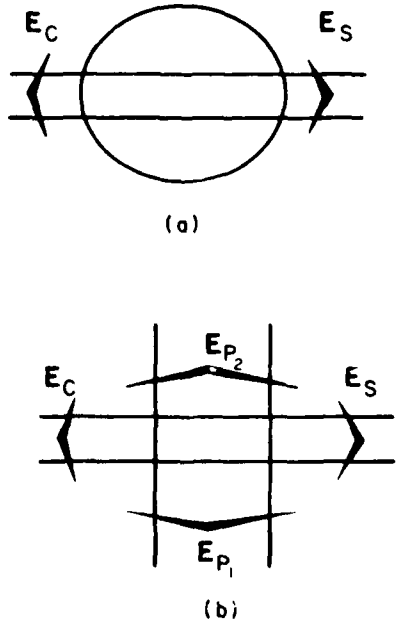

FIG. 1. (a) Side view illustration of the conjugate and signal fields cutting across the pump field profile. The conjugate and signal field profiles are assumed to be smaller than the pump profiles; in this limit only the z dependence of the pump profiles is important. (b) Top view illustration of the conjugate, signal, and pump fields.

coefficients $\alpha(z)$ can be transformed out of the equations by introducing a phase factor

$$\phi(z)=-\frac{1}{2k}\int_{-\infty}^{z}\alpha(z')dz' \tag{9}$$

and transforming the amplitudes

$$\begin{aligned}&\hat{E}_s\rightarrow\hat{E}_s e^{i\phi}\,,\\&\hat{E}c^*\rightarrow\hat{E}_c^* e^{i\phi}\,.\end{aligned} \tag{10}$$

The equations so generated can be used as the basis of further calculations on dynamic properties. However, the steady-state results in this paper already provide information about the response of the phase-conjugating mirror to different frequency components. Therefore, these results are relevant to describing the time-dependent fields.

The transverse modes are easily treated by introducing the Fourier transform of the transverse coordinates. Let the transverse wave number be $\eta^2=k_x^2+k_y^2$ and for comparison with other work we define $\beta(z)=2k\kappa G(z)$, where the integral of $G(z)$ is equal to unity. The coefficient κ is related to the space-averaged strength of the pump fields. Consider the signal to be detuned from the pump waves, the steady-state equations for the signal and conjugate fields are

$$\frac{dE_s}{dz}=\left[-i\Delta\frac{-i\eta^2}{F}\right]E_s-i\kappa G(z)E_c^* \tag{11a}$$

and

$$\frac{dE_c^*}{dz}=\left[i\Delta\frac{-i\eta^2}{F}\right]E_c^*-i\kappa G(z)E_s\,, \tag{11b}$$

where the z coordinate has been scaled to a characteristic length of the interaction region L; and the transverse coordinates have been scaled to the waist d, of the incoming signal. $F=2kd^2/L$ is the Fresnel number. Δ is the detuning of the signal from the pump fields and is scaled to nL/c. This is generated by the phase mismatch of the signal and conjugate field momenta. The caret has been dropped to denote the Fourier transform with respect to the transverse direction. The transverse coordinate can be removed by transforming the fields, and the equations can be combined into a single second-order differential equation for the complex fields. For instance, the signal field satisfies the equation

$$E_s''=\frac{G'}{G}E_s'-\left[\kappa^2G^2+\Delta^2-i\Delta\frac{G'}{G}\right]E_s\,, \tag{12}$$

where the primes denote a derivative with respect to z. Specific functions $G(z)$ are treated in the following section.

III. RESULTS

The second-order differential equation Eq. (12) of the previous section is useful for obtaining explicit solutions with detuning. We consider two cases here, the exponential pump profile:

$$G(z)=e^zH(-z)\,, \tag{13}$$

where $H(x)$ is the Heaviside function and the length scale of the exponential has already been included in the definition of z. This profile would be approximately realized experimentally by blocking all but a tail portion of the pump beams. Of course, combinations of exponentials, such as $\exp(-|z|)$ can be analytically treated, as well. The second case is the hyperbolic secant pump profile,

$$G(z)=\frac{1}{\pi}\operatorname{sech}(z)\,. \tag{14}$$

This profile simulates the transverse shape of a laser beam.

For comparison we use results for the square pump profile defined as

$$G(z)=[H(1-z)-H(-z)]\,. \tag{15}$$

In this case the coefficients of the differential equation are constant and the general solution for the signal field is

$$E_s(z)=\frac{E_s(0)\kappa^2\cos[\theta(1-z)]}{(\theta\cos\theta+i\Delta\sin\theta)}\,, \tag{16}$$

where $\theta^2=\kappa^2+\Delta^2$. This assumes that the conjugate field at $z=1$ vanishes, i.e., no conjugate signal is injected into the medium. The conjugate signal is

$$E_c^*(z)=-iE_s(0)\frac{\kappa^2\sin[\theta(1-z)]}{(\theta\cos\theta+i\Delta\sin\theta)}\,. \tag{17}$$

The dependence on η has not been included in the notation, but these results are valid for transverse signal and conjugate profiles within the limits imposed by the pump geometry, cf. Fig. 1. These solutions simplify to the well-known results:[9]

$$E_s(z)=E_s(0)\frac{\cos[\kappa(1-z)]}{\cos\kappa} \tag{18}$$

and

$$E_c^*(z)=-iE_s(0)\frac{\sin[\kappa(1-z)]}{\cos\kappa}\,. \tag{19}$$

The coupling coefficient κ is varied by changing the length of the interaction region in the pump field amplitudes in the region $\pi/4<\kappa<3\pi/4$, in which the signal and conjugate fields are amplified. Near $\kappa=\pi/2$ there is a so-called oscillation threshold where a small signal field value produces a large conjugate and signal field output. These spontaneous amplification regimes appear at higher values of κ as well, $\kappa=3\pi/2$, $5\pi/2$, etc. and are the result of fulfilling a resonance condition in the medium.

A. Exponential pump profile

Here we only treat the profile given by Eq. (13); however, it is also possible to solve for combinations of exponential pump shapes both rising and falling as functions of z. Equation (12) is solved for this case by transforming the coordinates to a new variable $\xi=e^z$. The resulting equation is

$$\frac{d^2E_s}{d\xi^2}+\left[\kappa^2+\frac{(\Delta^2-i\Delta)}{\xi^2}\right]E_s=0\,. \tag{20}$$

The solutions of this equation are related to Bessel functions[10]

$$E_s(\xi)=A\xi^{1/2}J_\nu(\kappa\xi)+B\xi^{1/2}J_{-\nu}(\kappa\xi)\ , \tag{21}$$

where $\nu=\frac{1}{2}+i\Delta$ is used in order to simplify the notation. The coefficients A and B are determined from the boundary conditions. The asymptotic form of the Bessel functions[10] is

$$J_\nu(z)\simeq\frac{(\frac{1}{2}z)^\nu}{\Gamma(\nu+1)}\ , \tag{22}$$

where $\Gamma(x)$ is the gamma function.[10]

As $\xi\to 0$, the signal field is

$$E_s(\xi)\simeq\left[\frac{2}{\kappa}\right]^\nu\frac{Be^{-i\Delta z}}{\Gamma(1-\nu)}\ . \tag{23}$$

This is the asymptotic form required of the signal field when the pump fields are turned off:

$$E_s(z)=E_s(0)e^{-i\Delta z}\ , \tag{24}$$

and the coefficient is

$$B=E_s(0)\left[\frac{\kappa}{2}\right]^\nu\Gamma(1-\nu)\ . \tag{25}$$

The secondary boundary condition is obtained at $\xi=1$ and is actually a boundary condition for the conjugate field. This field can be calculated from Eq. (11a); the result is

$$E_c^*(\xi)=+i\xi^{1/2}[AJ_{-\nu^*}(\kappa\xi)-BJ_{\nu^*}(\kappa\xi)]\ . \tag{26}$$

The conjugate field has its boundary at $\xi=1$ (or $z=0$) and the amplitude A is

$$A=\frac{\left[-iE_c^*(1)+E_s(0)\left[\frac{\kappa}{2}\right]^\nu\Gamma(1-\nu)J_{\nu^*}(\kappa)\right]}{J_{-\nu^*}(\kappa)}\ . \tag{27}$$

In phase conjugating experiments a conjugate field is not inserted in the medium $E_c^*(\xi=1)=0$. The solution for the phase conjugate field is

$$E_c^*(\xi)=-iE_s(0)\xi^{1/2}\left[\frac{\kappa}{2}\right]^\nu\Gamma(1-\nu)\times\left[J_{\nu^*}(\kappa\xi)-\frac{J_{\nu^*}(\kappa)}{J_{-\nu^*}(\kappa)}J_{-\nu^*}(\kappa\xi)\right]\ . \tag{28}$$

The solution for the field when the signal is degenerate with the pumps ($\Delta=0$) is

$$E_c^*(\xi)=-i\frac{\sin[\kappa(1-\xi)]}{\cos\kappa}E_s(0)\ . \tag{29}$$

This solution has properties which are similar to those derived by assuming that the pump beams have a constant amplitude profile which falls abruptly to zero. For intermediate pump field amplitudes, i.e., $\pi/4<\kappa<\frac{1}{4}\pi$, the phase-conjugate field is amplified in the medium, when the signal field is degenerate with the pumps. In this regime the reflectivity of the device is greater than unity. Furthermore, the intensities diverge for $\kappa=\pi/2$. This is a regime where the pumps would be depleted in order to keep amplifying the conjugate wave and spontaneous amplification of the signal occurs. Further regimes for spontaneous amplification appear near $\kappa=3\pi/2,\ 5\pi/2$, etc.

For $\Delta\neq 0$, the zeros of the Bessel function $J_{-\nu^*}(\kappa)$ lie off the real axis and the divergence is prevented. For pulses this means that not all frequency components of the conjugate wave are equally amplified. The field will be distorted for the conjugate wave, not only in its amplitude, but also in its phase. Similar properties are observed for the square profile as well, but there are large quantitative differences which will be discussed at the end of this section.

B. Hyperbolic secant pump profile

The differential equation for the signal amplitude is simplified by introducing the transformation

$$\xi=\frac{1+\tanh(z)}{2}\ . \tag{30}$$

The equation is

$$\xi(1-\xi)\frac{d^2E_s}{d\xi^2}+\frac{(1-2\xi)}{2}\frac{dE_s}{d\xi}+\left[\frac{\kappa^2}{\pi^2}-i\Delta\frac{(1-2\xi)}{4\xi(1-\xi)}+\frac{\Delta^2}{4\xi(1-\xi)}\right]E_s=0\ . \tag{31}$$

This equation has the structure of the Riemannian differential equation and the solution of Eq. (31) can be expressed in terms of hypergeometric functions[10] ${}_2F_1(a,b;c;z)$:

$$E_s(\xi)=\left[\frac{\xi}{\xi-1}\right]^{-i\Delta/2}\times\left[A\,{}_2F_1\left[\frac{\kappa}{\pi},\frac{-\kappa}{\pi};\nu^*;\xi\right]+B\xi^\nu\,{}_2F_1\left[\frac{\kappa}{\pi}+\nu,\frac{-\kappa}{\pi}+\nu;1+\nu;\xi\right]\right] \tag{32}$$

as $\xi\to 0$ (i.e., $z\to-\infty$). The asymptotic solution is

$$E_s(\xi)=(-\xi)^{-i\Delta}A\ . \tag{33}$$

This conforms with the proper asymptotic solution of the free field $E_s(z)$ which is

$$E_s(z)=E_s(0)e^{-i\Delta z}\ . \tag{34}$$

The coefficient A is

$$A=E_s(0)(-1)^{(i\Delta/2)}\ . \tag{35}$$

The phase-conjugate field is

$$E_c(\xi)=\frac{-i\pi}{\kappa}\left[\frac{\xi}{\xi-1}\right]^{(-i\Delta/2)}\sqrt{\xi(1-\xi)}\left[\frac{E_s(0)(-1)^{(i\Delta/2)}}{\nu^*}\left[\frac{\kappa}{\pi}\right]^2(1-\xi)^{-\nu}{}_2F_1\left[\nu^*-\frac{\kappa}{\pi},\nu^*+\frac{\kappa}{\pi};1+\nu^*;\xi\right]\right.$$
$$-B\left[\nu\xi^{-\nu^*}{}_2F_1\left[\frac{\kappa}{\pi}+\nu,\frac{-\kappa}{\pi}+\nu;1+\nu;\xi\right]\right.$$
$$\left.\left.+\left\{\left[\nu^2-\left[\frac{\kappa}{\pi}\right]^2\right]\Big/(1+\nu)\right\}\xi^{\nu}{}_2F_1\left[1+\frac{\kappa}{\pi}+\nu,1-\frac{\kappa}{\pi}+\nu;2+\nu;\xi\right]\right\}\right] \tag{36}$$

The boundary condition for the conjugate field applies at $\xi=1$. After some algebra the coefficient B is

$$B=\left[\frac{-i\kappa}{\pi}E_c^*(1)(-1)^{-i\Delta/2}+\left[\frac{\kappa}{\pi}\right]^2\frac{(-1)^{i\Delta/2}}{\nu^*}E_s(0)\,{}_2F_1\left[-\frac{\kappa}{\pi}+\nu^*,\frac{\kappa}{\pi}+\nu^*;1+\nu^*;1\right]\right]$$
$$\times\left\{(1+\nu)\left[\nu^2-\left[\frac{\kappa}{\pi}\right]^2\right]\right\}{}_2F_1\left[1-\frac{\kappa}{\pi},1+\frac{\kappa}{\pi};2+\nu;1\right]. \tag{37}$$

The amplification of the fields resonant with the pump fields occur at the same values of κ as in the previous examples of a square profile and an exponential pump profile. The spontaneous amplification regimes appear at the zeros of the function[10]

$$\left[\frac{1}{4}-\left[\frac{\kappa}{\pi}\right]^2\right]{}_2F_1\left[1-\frac{\kappa}{\pi},1+\frac{\kappa}{\pi};\frac{5}{2};1\right]=\left[\frac{1}{4}-\left[\frac{\kappa}{\pi}\right]^2\right]\frac{\Gamma\left[\frac{5}{2}\right]\Gamma\left[\frac{1}{2}\right]}{\Gamma\left[\frac{3}{2}+\frac{\kappa}{\pi}\right]\Gamma\left[\frac{3}{2}-\frac{\kappa}{\pi}\right]}. \tag{38}$$

The divergences of the gamma function $\Gamma(3/2-\kappa/\pi)$ can also be found in Ref. 10; they also appear at $\kappa=3\pi/2$, $5\pi/2$, etc.

C. General result for resonant fields

The fact that all of the above profiles have identical values for the divergences suggest that a general theorem holds for classes of pump profile shapes. This is indeed the case and is derived in the following.

For a transverse profile $G(z)\geq 0$, we define the area as

$$q(z)=\int_{-\infty}^{z}G(z')dz'. \tag{39}$$

Equation (11) for $\Delta=0$ can be transformed to

$$\frac{dE_s}{dq}=-i\kappa E_c^* \tag{40a}$$

and

$$\frac{dE_c^*}{dq}=-i\kappa E_s \tag{40b}$$

as long as $q(z)$ is *monotonic*.

The solution of this case is precisely the square profile, Eqs. (18) and (19):

$$E_s(q)=E_s(0)\frac{\cos[\kappa(q-1)]}{\cos\kappa} \tag{41a}$$

and

$$E_c^*(q)=-iE_s(0)\frac{\sin[\kappa(1-q)]}{\cos\kappa}. \tag{41b}$$

The spontaneous amplification regimes appear at identical values of κ independent of the profile shape. In particular the Gaussian-shaped profiles will likewise obey this threshold condition.

D. Numerical illustration

To illustrate these results in greater detail the intensities are plotted for the three pump profiles. The signal fields are shown in Fig. 2 for $\kappa=0.78$. The longitudinal coordinate extends over the range [0,1]; for the square pump profile this coordinate is the z axis and for the exponential and hyperbolic secant pump profiles the scaled variable ξ is used for this coordinate. The profiles of the intensities are plotted versus detuning from the pump resonance; for convenience this is scaled as a square root. A constant field $E_s(0)$ is used in the calculations; this allows a simple interpretation of the results for inhomogeneous dependence of $E_s(0)$ on the detuning.

For the square profile the amplitude difference between $\Delta=\pm 4$ and 0 is about a factor of 5 when the coupling constant is $\kappa=0.78\simeq\pi/4$. The signal field is amplified over the entire output ($z=1$) for the range of detunings shown. For the exponential profile, Fig. 2(b), and the hyperbolic secant profile, Fig. 2(c), the wings of the signal intensity at $\Delta=\pm 4$ are not amplified at all at the output $\xi=1$. The exponential profile gives a broader frequency response than the hyperbolic-secant profile.

The conjugate intensities exhibit a corresponding response to the pump profiles; comparison between Figs. 2(a) and 3(a) reveal that the reflectivity is also amplified in the entire detuning region shown. This is contrast with

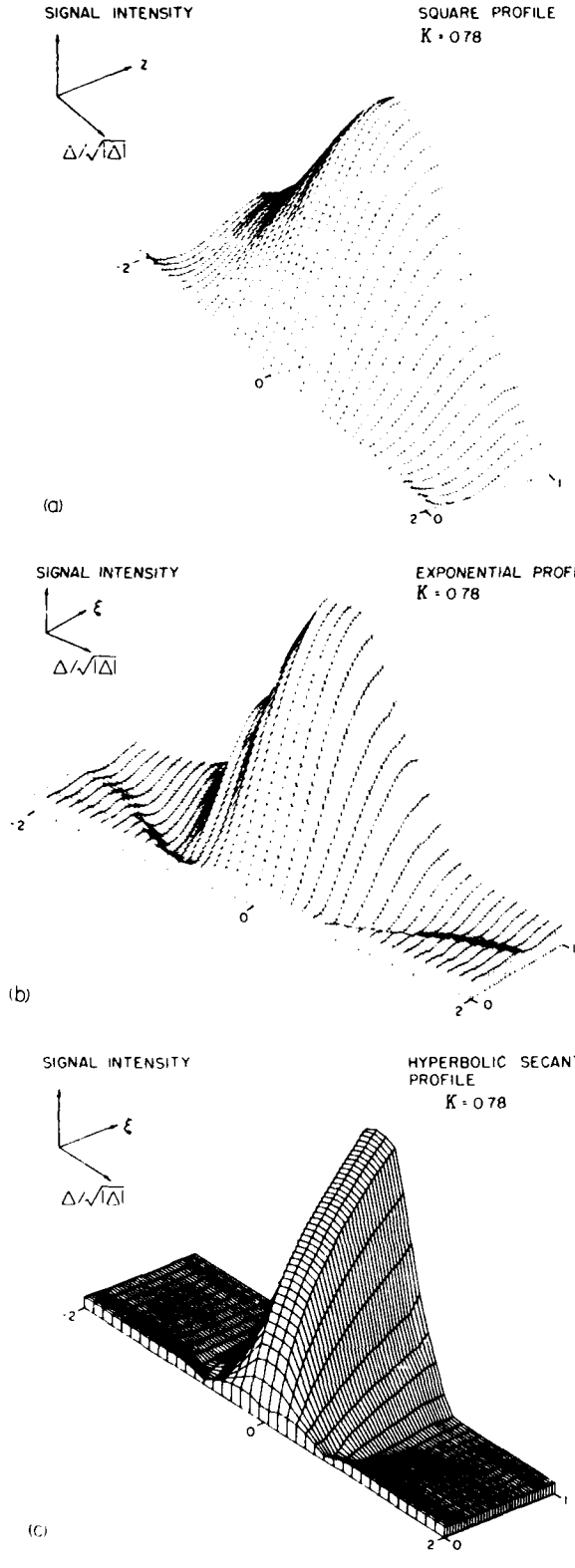

FIG. 2. (a) The signal intensity resulting from an interaction with a square pump profile. The three-dimensional representation. The value of the coupling constant is $\kappa = 0.78$. The z axis is shown and the square root of the detuning times the signum of the detuning. (b) As in (a), except that the exponential pump profile is used and the ξ axis is plotted. (c) As in (b), but for the hyperbolic secant pump profile.

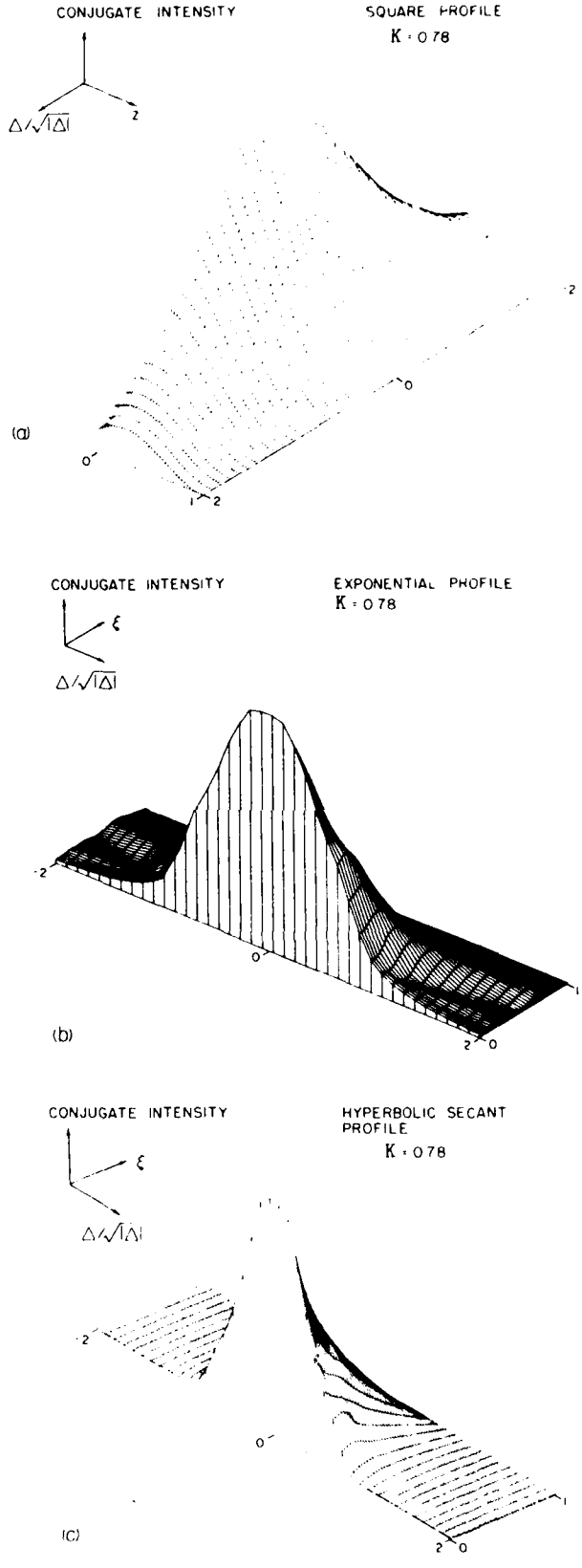

FIG. 3. (a) Conjugate intensity corresponding to Fig. 2(a). (b) Conjugate intensity corresponding to Fig. 2(b). (c) Conjugate intensity corresponding to Fig. 2(c).

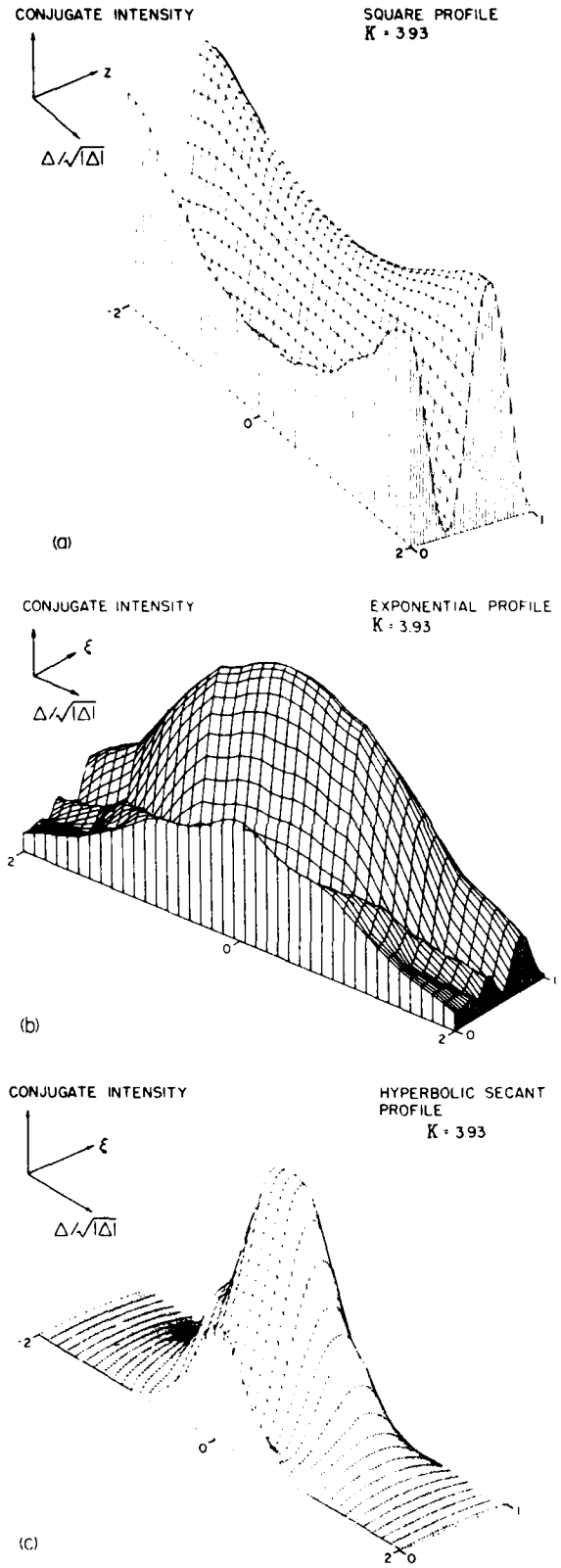

FIG. 4. (a) Conjugate intensity for the square pump profile, all parameters as in Fig. 2(a) with the coupling coefficient $\kappa = 3.93$. (b) Conjugate intensity for the exponential pump profile $\kappa = 3.93$. (c) Conjugate intensity for the hyperbolic-secant pump profile $\kappa = 3.93$.

the results of Figs. 3(b) and 3(c) which clearly demonstrate the inability of the smooth pump profiles to interact with fields which have a large detuning. Again the exponential profile has a wider conjugate field response to the signal field than the hyperbolic secant profile.

From Eq. (17), it is obvious that the response of the conjugate fields is more uniform when the coupling constant is larger. At least this is the case for a square profile. This is indeed the case for the conjugate field shown in Fig. 4(a). Here the coupling constant was chosen as $\kappa = 3.93 \simeq 5\pi/4$. The central region is amplified less than the wings $\Delta = \pm 4$ and the difference in amplification is now only about a factor of 2. The larger coupling constants also give more structure to the fields in the medium. This also could be anticipated from Eq. (29). The conjugate intensity from the exponential pump profile is also broadened from $\kappa = 3.93$, Fig. 4(b). However, for the hyperbolic secant pump profile, the detuning response of the conjugate field has not been significantly increased for this value of the coupling constant, Fig. 4(c). The wings for $|\Delta| > 1$ are not responding to the pump profile.

IV. CONCLUSIONS

In view of the foregoing results, several remarks are worth mentioning. In noncritical situations where the bandwidth of the signal is small compared to c/nL the conjugate field is a good time-reversed replica of the incoming signal. This means that the precise profile of the pumps are not a determining factor in achieving good optical phase conjugation fidelity.

As the bandwidth is increased the amount of loss of fidelity depends sensitively on the pump profile shape. We find that the square pump profiles [Figs. 3(a) and 4(a)] have better fidelity than the exponential and the hyperbolic secant pump profiles. These results could be tested, for instance, using an experimental arrangement similar to Falk;[11] he tested the fidelity of phase conjugation using CS_2 with a 1-cm path length and the same DFWM geometry discussed here. Only millijoules of energy are required for the pump beams and the detuning of the signal required to observe the effects discussed here is about 20 GHz.

Of course, there is one caveat to this which is not exhibited in the figures, namely, the phase of the conjugate fields is also distorted by the frequency detuning of the signal field from the pump fields. For the square pump profiles the phase distortion can also be minimized by increasing the coupling constant, i.e., increasing pump intensities, cf. Eq. (17). The phase distortion correction of the exponential and hyperbolic secant pump profiles for large κ are not as obvious, but analogous to the discussion of the intensities in the preceding section, we find that the square profile has the best distortion correction and the hyperbolic-secant profile the worst. The phase reversal is rapidly improved as the pump widths are decreased;[5] however, the smooth pump profiles ability to correct the phase distortions is reduced.

If we interpret the trends shown in Figs. 3 and 4 and discussed above, then the pump profiles with sharp edges

produce higher quality phase conjugation than those with smooth profiles. The pump profiles could provide a barrier to developing phase conjugation devices for very fast signal processing with a minimal loss of fidelity. The bandwidth can be increased by using smaller pump profiles.

ACKNOWLEDGMENTS

J. W. Haus was supported by the U.S. Army Research Office, Department of the Army under Contract No. DAAG29-81-D-0100. C.C.S. and J.W.H. were partially supported by National Science Foundation Grant No. ECE-841530.

[1]For a compreshensive treatment, see *Optical Phase Conjugation*, edited by R. A. Fisher (Academic, New York, 1983).

[2]F. A. Hopf, J. Opt. Soc. Am. **10**, 1320 (1980).

[3]M. D. Ewbank, P. Yeh, M. Khoshnevisan, and J. Feinberg, Opt. Lett. **10**, 282 (1985).

[4]D. M. Pepper, J. Au Young, D. Fekete, and A. Yariv, Opt. Lett. **3**, 7 (1978); T. R. O'Meara and A. Yariv, Opt. Eng. **21**, 237 (1982).

[5]R. A. Fisher, B. R. Suydam, and B. J. Feldman, Phys. Rev. A **23**, 3071 (1981); W. W. Rigrod, R. A. Fisher, and D. M. Pepper, Opt. Lett. **5**, 105 (1980); B. R. Suydam and R. A. Fisher, Opt. Eng. **21**, 184 (1982).

[6]D. M. Pepper and R. L. Abrams, Opt. Lett. **3**, 212 (1978); B. Crosignani and P. DiPorto, *ibid.* **7**, 489 (1982).

[7]Y. Silberberg and I. Bar-Joseph, IEEE J. Quantum Electron **QE-17**, 1967 (1981).

[8]See, for instance, H. Haken, *Laser Theory* (Springer, Berlin, 1984).

[9]D. M. Bloom and G. C. Bjorklund, Appl. Phys. Lett. **31**, 592 (1977); A. Yariv and D. M. Pepper, Opt. Lett. **1**, 16 (1977).

[10]M. Abramowitz and I. A. Stegun, *Handbook of Mathematical Functions* (Dover, New York, 1968).

[11]J. Falk, Opt. Lett. **7**, 620 (1982).